

## SUPPLEMENTAL INFORMATION

15 supplemental figures, 1 supplemental table and supplemental methods

### **The *PTPN22* risk variant promotes systemic autoimmunity in murine models**

Xuezhi Dai<sup>1,7</sup>, Richard G. James<sup>3</sup>, Tania Habib<sup>8</sup>, Swati Singh<sup>1,7</sup>, Shaun Jackson<sup>1,7</sup>, Socheath Khim<sup>1,7</sup>, Randall T. Moon<sup>3,6</sup>, Denny Liggitt<sup>4</sup>, Alejandro Wolf-Yadlin<sup>5</sup>, Jane H. Buckner<sup>8</sup>, David J Rawlings<sup>1,2,7</sup>

Departments of Pediatrics<sup>1</sup>, Immunology<sup>2</sup>, Pharmacology<sup>3</sup>, Comparative Medicine<sup>4</sup> and Genome Sciences<sup>5</sup>, and Howard Hughes Medical Institute<sup>6</sup>, University of Washington School of Medicine, Seattle, WA 98195

Seattle Children's Research Institute<sup>7</sup> and Translational Research Program<sup>8</sup>, Benaroya Research Institute, Seattle, WA, 98101, USA

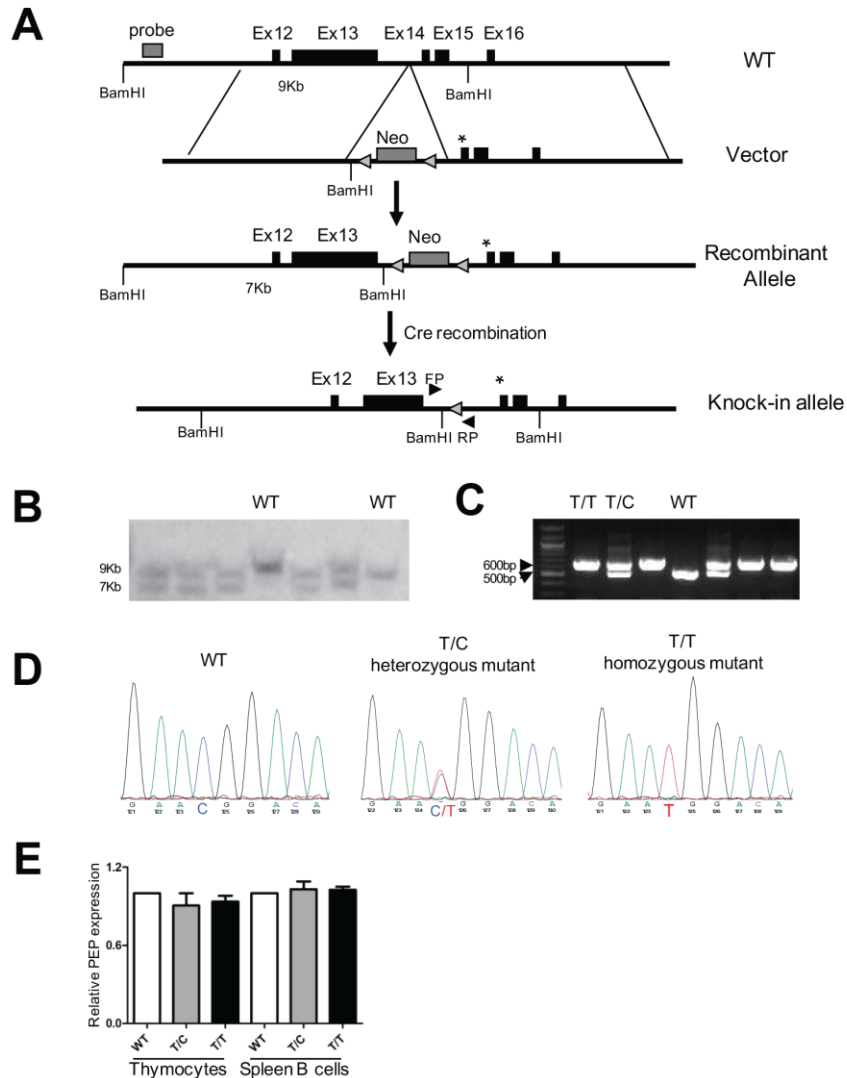
#### **Correspondence:**

David J. Rawlings, M.D., Center for Immunity and Immunotherapies, Seattle Children's Research Institute, 1900 Ninth Avenue, Seattle, WA 98101

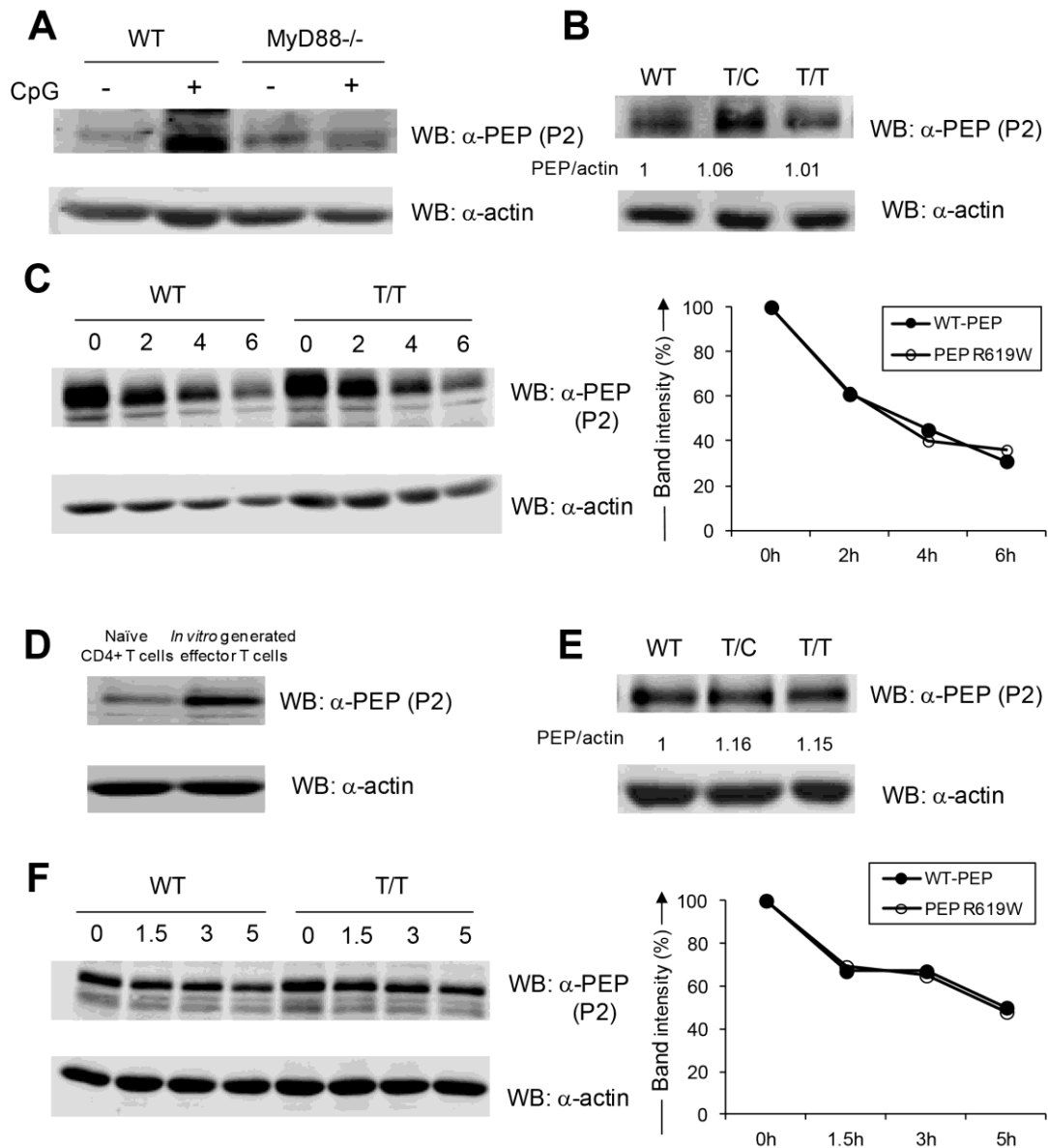
Tel. (206) 987-7450

Fax (206) 987-7310

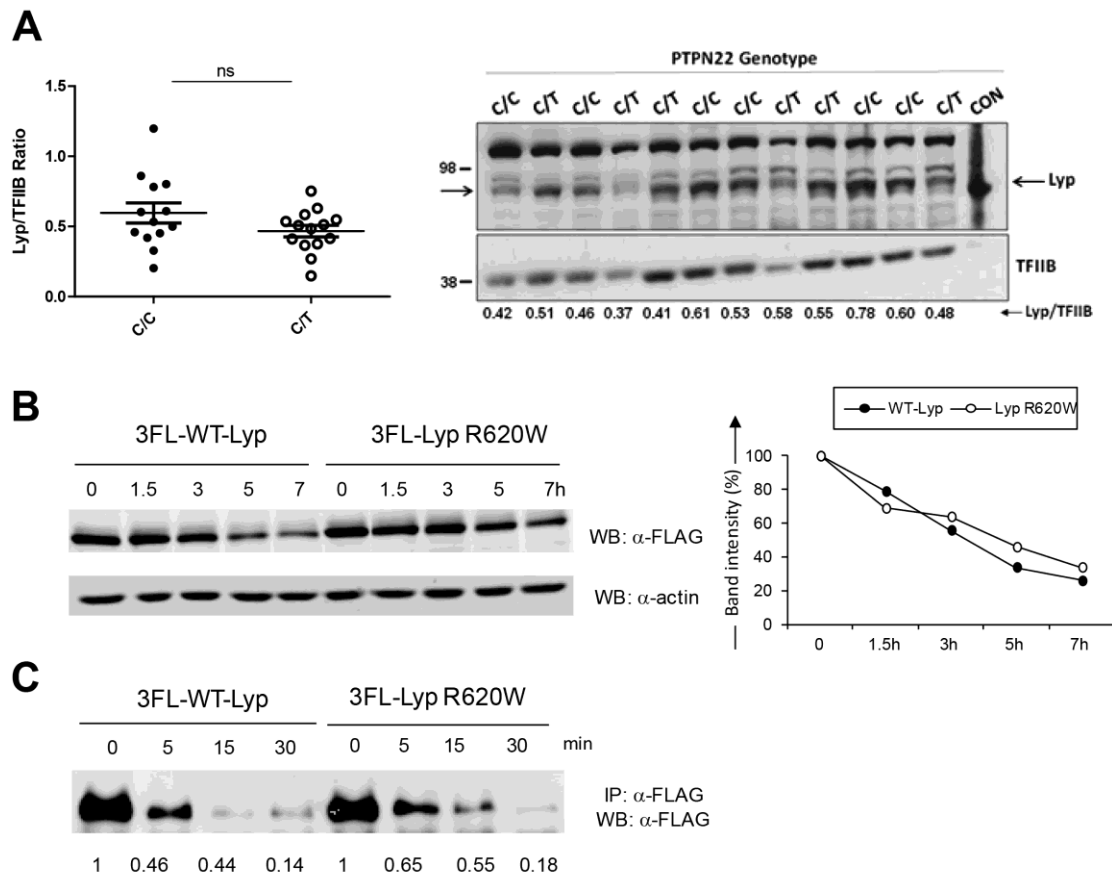
E-mail: [drawling@u.washington.edu](mailto:drawling@u.washington.edu)



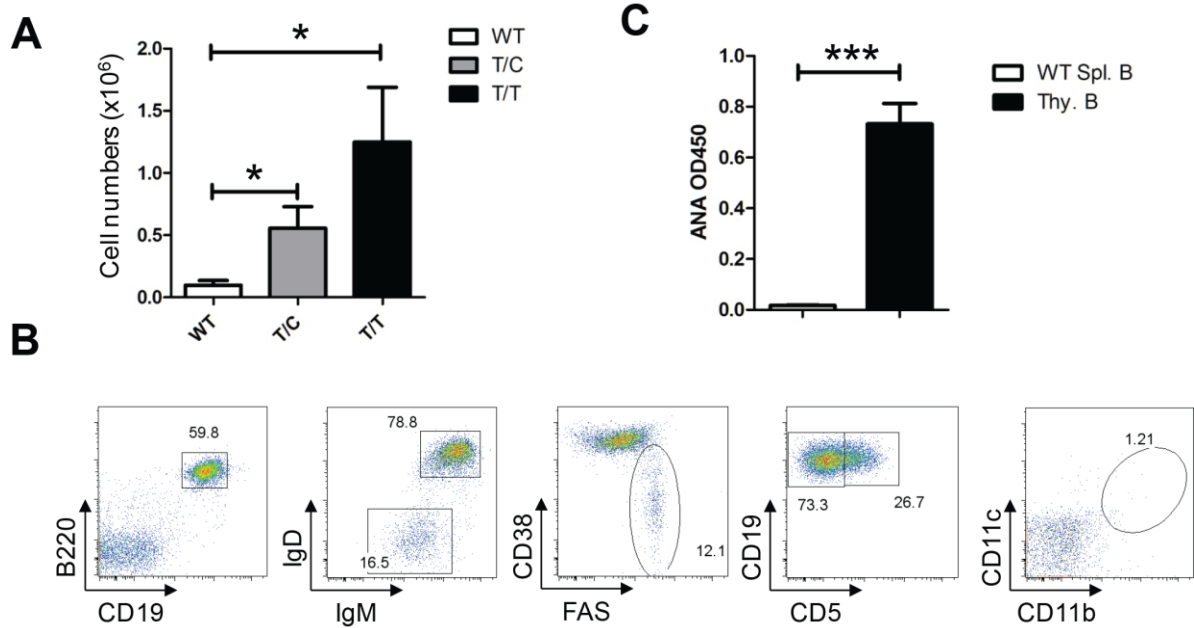
**Supplemental Figure 1. Generation of PEP-R619W knock-in mice.** (A) Strategy for generating the PEP-R619W knock-in mice. (B) Southern blot of BamHI digests showing positive ES cell clones. The probe for Southern blot is indicated. The lower band (7kb) represents the correctly targeted ES cell clones. (C) Genotyping of tail genomic DNA from WT, T/C and T/T mice by PCR amplification using forward and reverse primers, FP and RP, indicated in (A). The WT allele corresponds to the lower band (482bp) and the knock-in allele to the upper band (640bp). (D) Validation of R619W mutation in T/C and T/T mice. The WT coding sequence is CGG (Arg) and the knock-in is TGG (Trp). (E) Expression of *Ptpn22* mRNA in thymus and purified splenic B cells from WT, T/C and T/T mice by Q-PCR. Data shown is representative of five (D) and two (E) independent experiments.



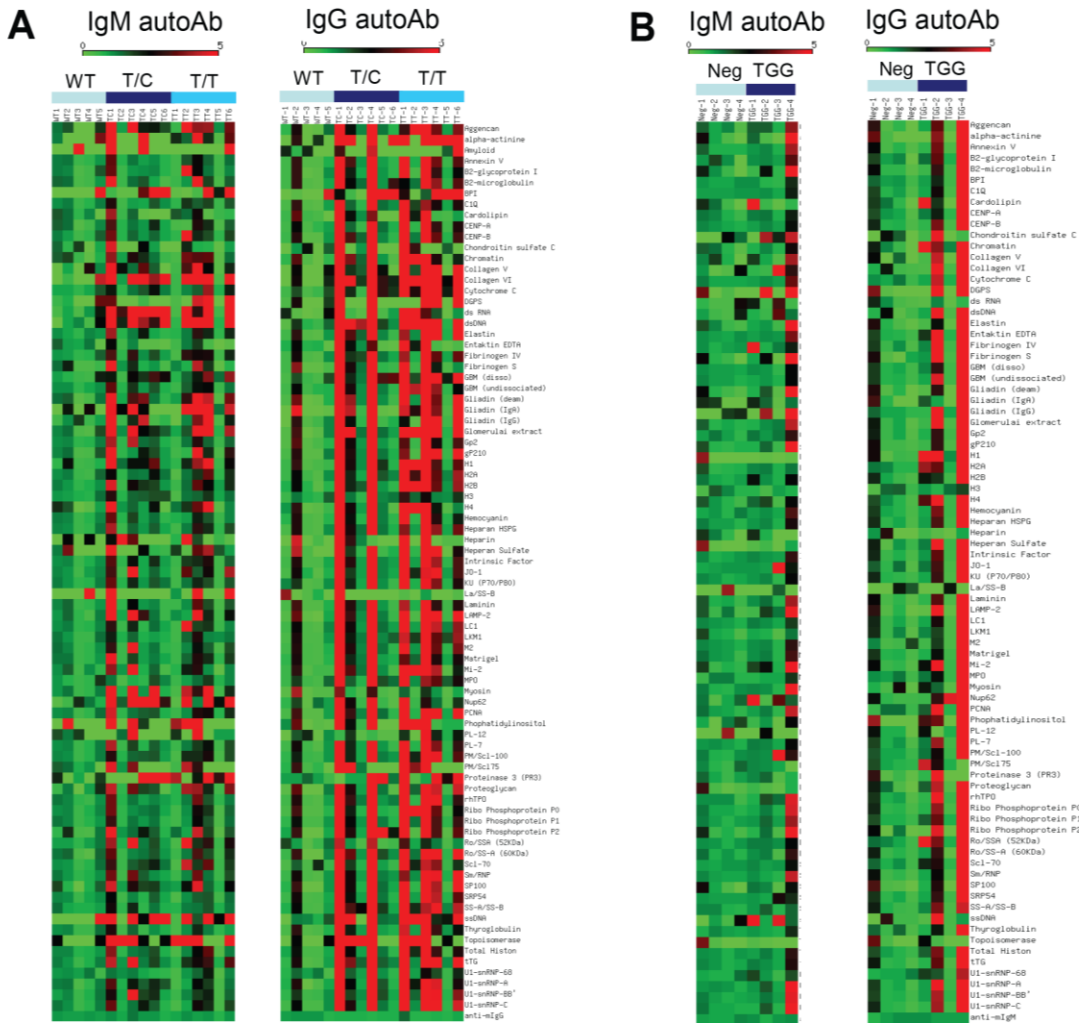
**Supplemental Figure 2. PEP-R619W exhibits no alteration in protein stability.** Increased PEP expression in CpG pre-stimulated B cells (A) and *in vitro* generated effector T cells (D). (B,E) PEP-R619W variant cells exhibit intact PEP up-regulation. Total cell lysates from CpG pre-stimulated B cells (B) or *in vitro* generated effector T cells (E) were subjected to western blot analysis with anti-PEP P2 and anti-actin antibodies. Numbers denote PEP/actin ratios. (C, F) Analysis of PEP half-life in CpG pre-stimulated B cells (C) and *in vitro* generated effector T cells (F). Cells were treated with 50 $\mu$ M cycloheximide for indicated times and cell lysates were blotted using anti-PEP-P2 and anti-actin antibodies. Graphic displays relative band intensity (PEP to actin) vs. time (right panel). Data shown is representative of at least two independent experiments.



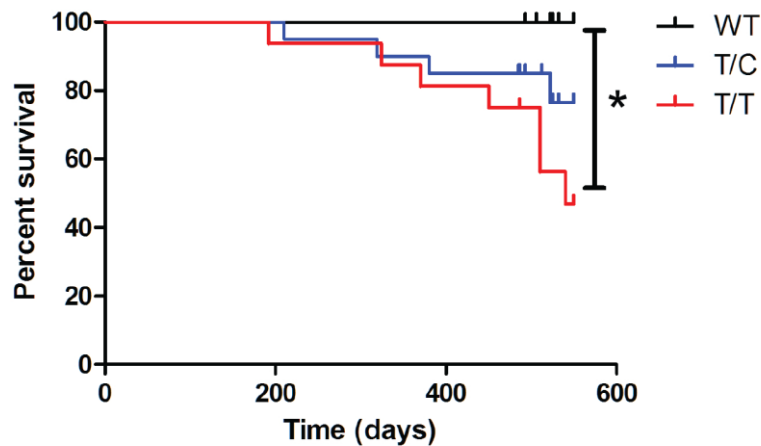
**Supplemental Figure 3. LYP-R620W exhibits no alteration in protein stability.** (A) Comparable LYP expression in purified CD3<sup>+</sup> T cells derived from peripheral blood mononuclear cells from *PTPN22* heterozygous variant (C/T) and control (C/C) subjects. Total cell lysates were subjected to Western blot analysis with anti-LYP and anti-TFIIB antibodies (right panel). 293T cells overexpressing LYP were used as a positive control. Left panel displays the LYP/TFIIB ratios with each symbol designating an individual subject. (B) Analysis of LYP half-life in Ramos B cells overexpressing FLAG-tagged LYP or LYP-R620W. Cells were treated with 50 $\mu$ M cycloheximide for indicated times and cell lysates were blotted using anti-FLAG and anti-actin antibodies. Graphic displays relative band intensity vs. time (right panel). (C) LYP and LYP-R620W exhibit similar calpain-1 mediated protein degradation. Cell lysates from Ramos B cells overexpressing FLAG-tagged LYP and LYP-R620W were immunoprecipitated with anti-FLAG antibody. The immunoprecipitates were incubated with 0.05U calpain-1 for indicated times and then subjected to Western blot analysis with anti-FLAG antibody. Numbers denote protein degradation rate. Data shown is representative of at least two independent experiments.



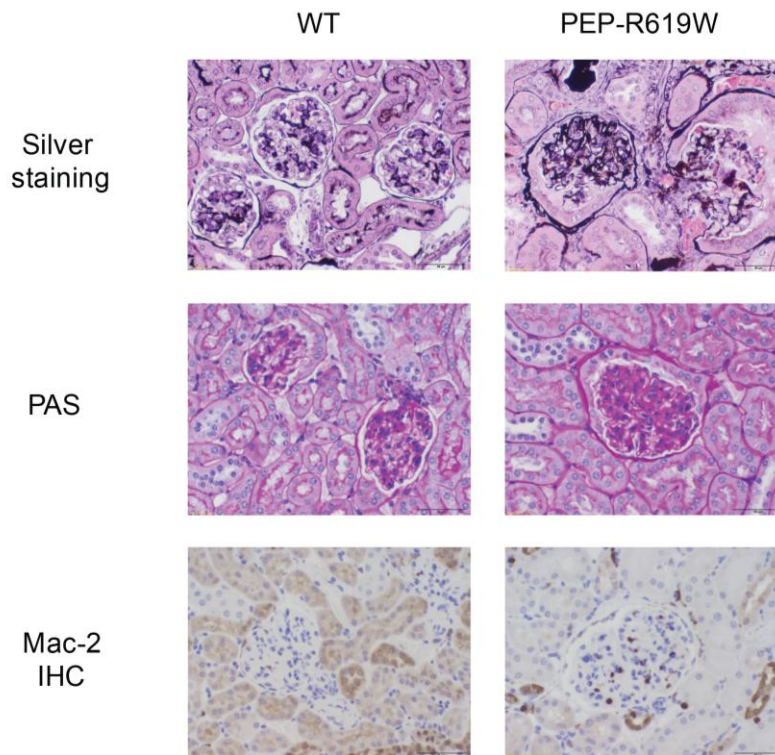
**Supplementary Figure 4. Characterization of thymic B cells in aged PEP-R619W knock-in mice.** (A) Absolute B cell numbers in thymus in aged (6-10 mo) T/C, T/T and WT littermates. Error bars depict standard deviation based on eight mice/ genotype; \*  $p < 0.05$ . (B) Representative cell surface phenotype of thymic B cells in aged PEP-R619W knock-in mice. Thymus derived cells were analyzed by FACS for CD4, CD8, B220, CD19, IgD, IgM, CD38, FAS, CD5, CD11b and CD11c expression. Data shown is representative of three independent experiments. (C) Thymic B cells from aged PEP-KI mice spontaneously produce anti-nuclear antibodies. Purified thymic B cells from aged PEP-KI mice and control splenic B cells from WT mice were cultured in RPMI media containing 10% FBS for 4 days. Supernatants were subjected to ANA Ig ELISA. Error bars depict standard deviation (3 mice/genotype); \*\*\*  $p < 0.001$ .



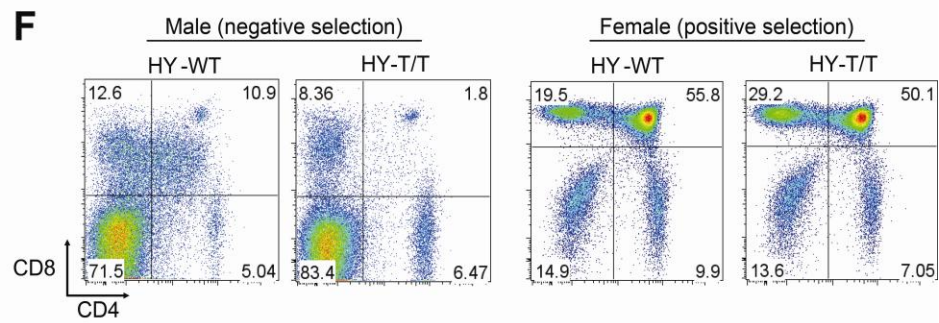
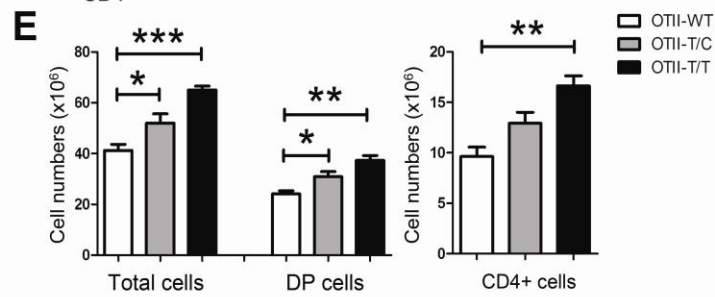
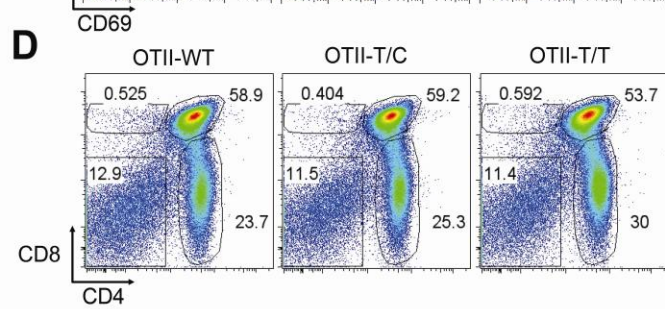
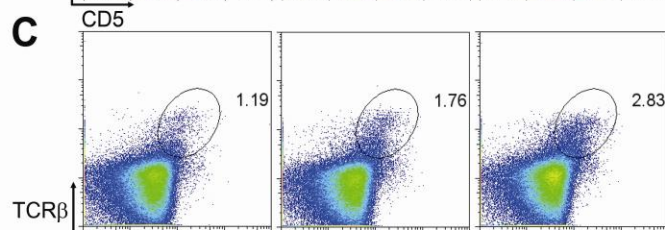
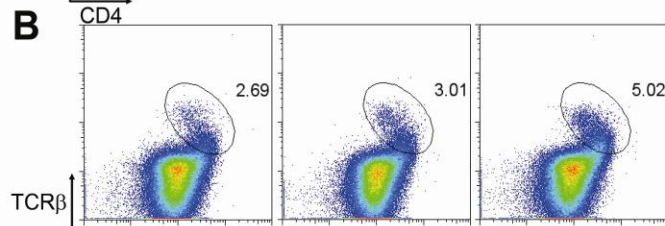
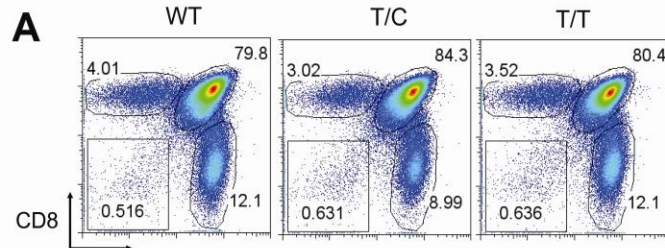
**Supplemental Figure 5. Aged knock-in mice and Rosa-PEP-R619W/CD19-Cre develop a broad range of autoantibodies.** Autoantigen arrays containing >70 autoantigens implicated in various human autoimmune diseases were used to identify IgM and IgG autoantibodies. (A) Analysis using sera from 6 mo littermate control (5 animals), T/C (6 animals), and T/T (6 animals) mice; (B) Analysis using sera from 10 mo of CD19-Cre and Rosa-PEP-R619W/CD19-Cre mice (4 animals each). Red squares in the array indicate  $\geq 5$ -fold increase in antibody titer compared to average values in control sera.



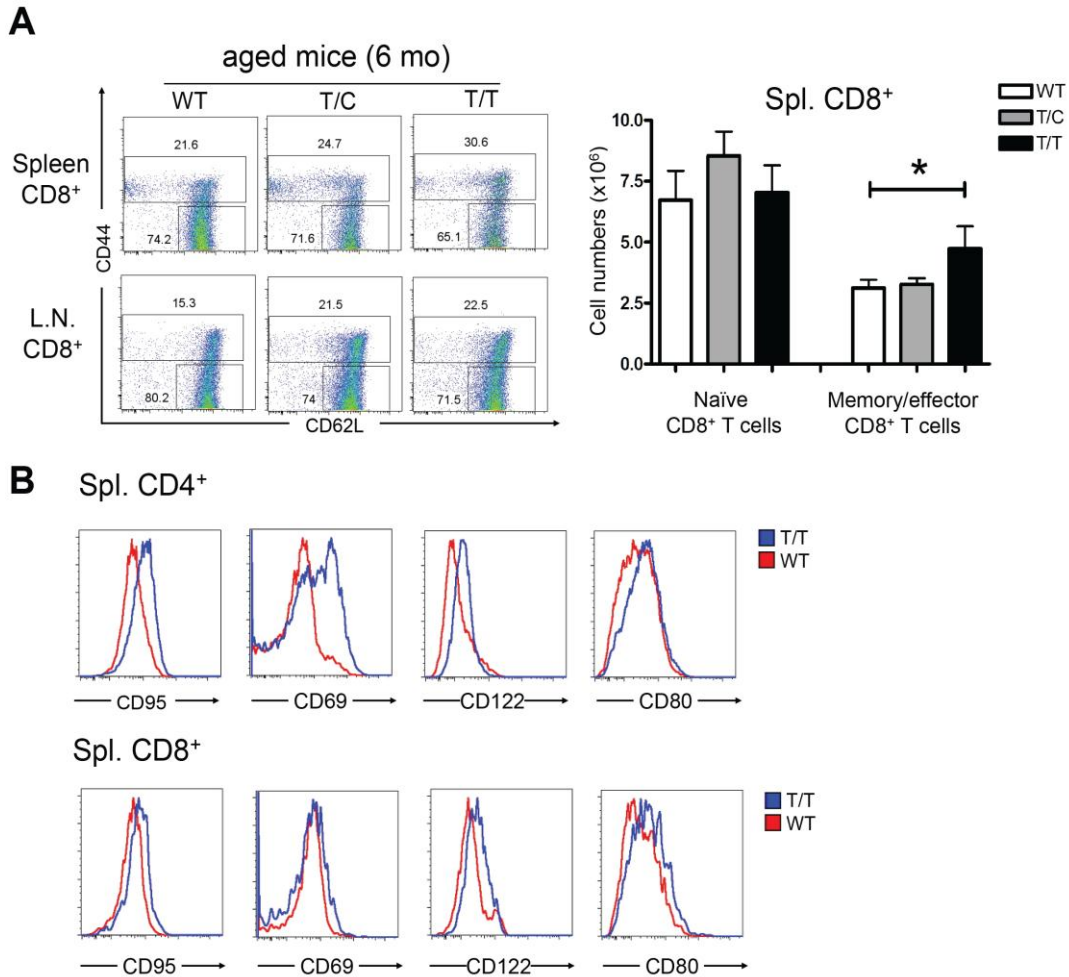
**Supplementary Figure 6. PEP R619W knock-in mice exhibit a reduced life-span.** Kaplan-Meier survival curve of WT ( $n = 17$ ), T/C ( $n=25$ ) and T/T ( $n=18$ ). \*  $p<0.05$ . Statistical significance of comparisons was assessed by log-rank (Mantel-Cox) test using GraphPad software.



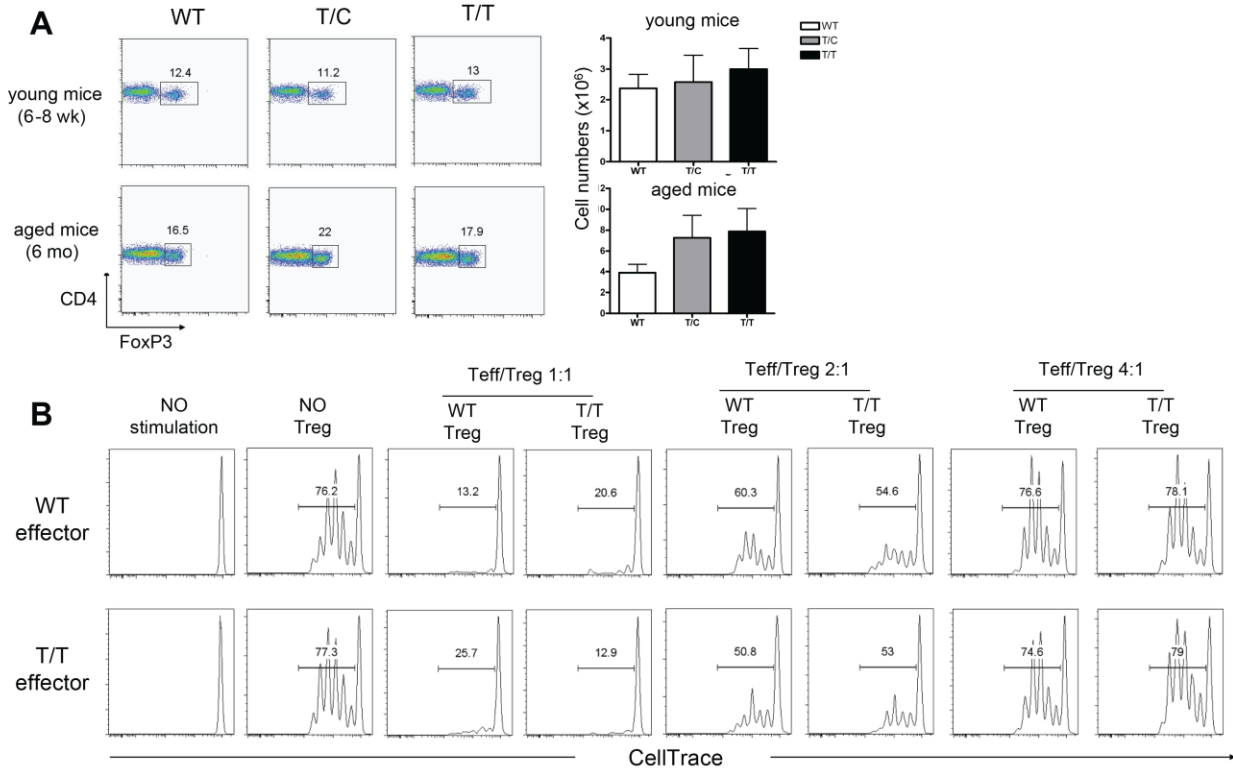
**Supplementary Figure 7. Aged knock-in mice develop modest renal glomerular injury.** Representative histopathology studies of kidneys from 10 mo WT and PEP-R619W knock-in mice showing increased glomerular cellularity and mesangial matrix (right panels, Silver and PAS stains) and glomerular infiltration of Mac-2<sup>+</sup> cells [right panel, Mac-2 immunohistochemistry (IHC)]. Scale bars: 50 $\mu$ m. Data shown are representative of findings from 3 WT, 4 T/C and 4 T/T mice.



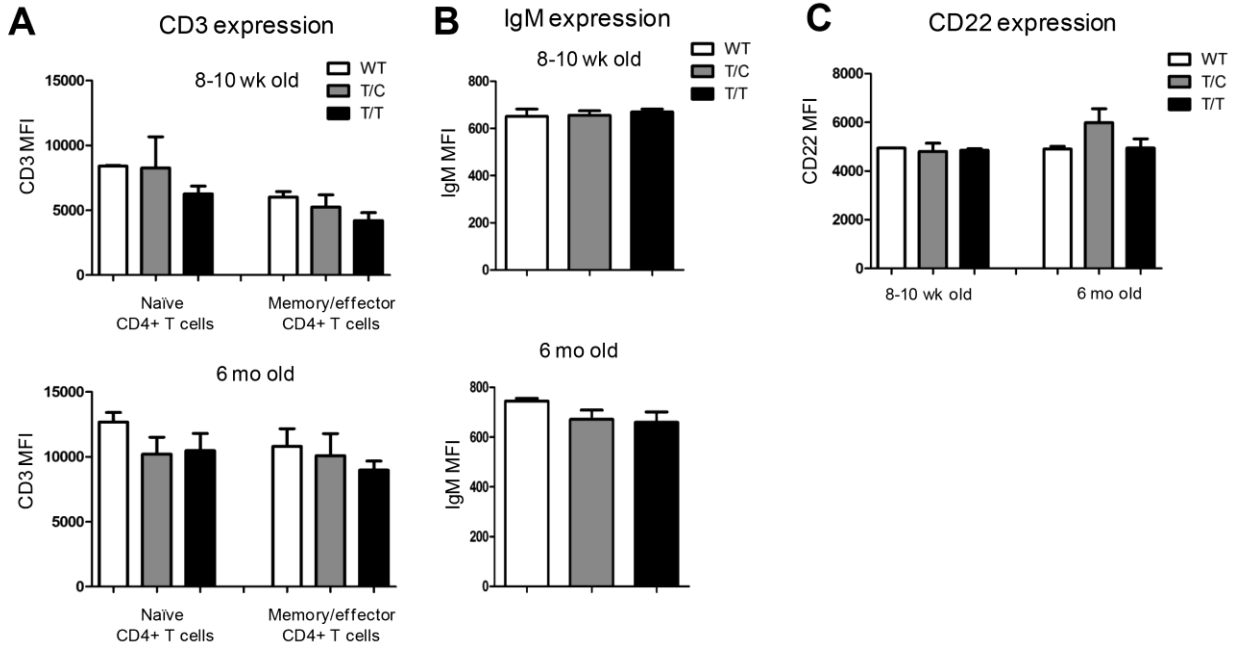
**Supplemental Figure 8. Enhanced thymic positive and negative selection in PEP-R619W knock-in mice.** (A) Comparable thymic T cell development in 6-8 wk old T/C, T/T and littermate control mice. Total thymocytes were analyzed by FACS using anti-CD4 and -CD8 staining. Percentages indicate events within the live cell gate. (B,C) Increased TCR $\beta^+$  CD5 $^+$  and TCR $\beta^+$  CD69 $^+$  cells within the CD4 $^+$  CD8 $^+$  DP thymocyte population. (D,E) Enhanced thymic positive selection in T/C, T/T and littermate control OT-II transgenic mice. (D) Total thymocytes in each strain were analyzed by FACS using anti-CD4 and -CD8 staining. Percentages indicate events within the live cell gate. (E) Absolute number of total thymocytes, CD4 $^+$  CD8 $^+$  (DP) cells and CD4 $^+$  single positive cells. Error bars represent standard deviation (5 mice/genotype). \* p<0.05; \*\* p<0.01; \*\*\* p<0.001. (F) Enhanced negative and positive selection in HY-PEP-R619W knock-in male and female mice, respectively. Total thymocytes in male (left) or female (right) were analyzed by FACS using anti-CD4 and -CD8 staining. Percentages indicate events within the live cell gate. Data shown are representative of six (A), three (B, C, F) and five (D) independent experiments.



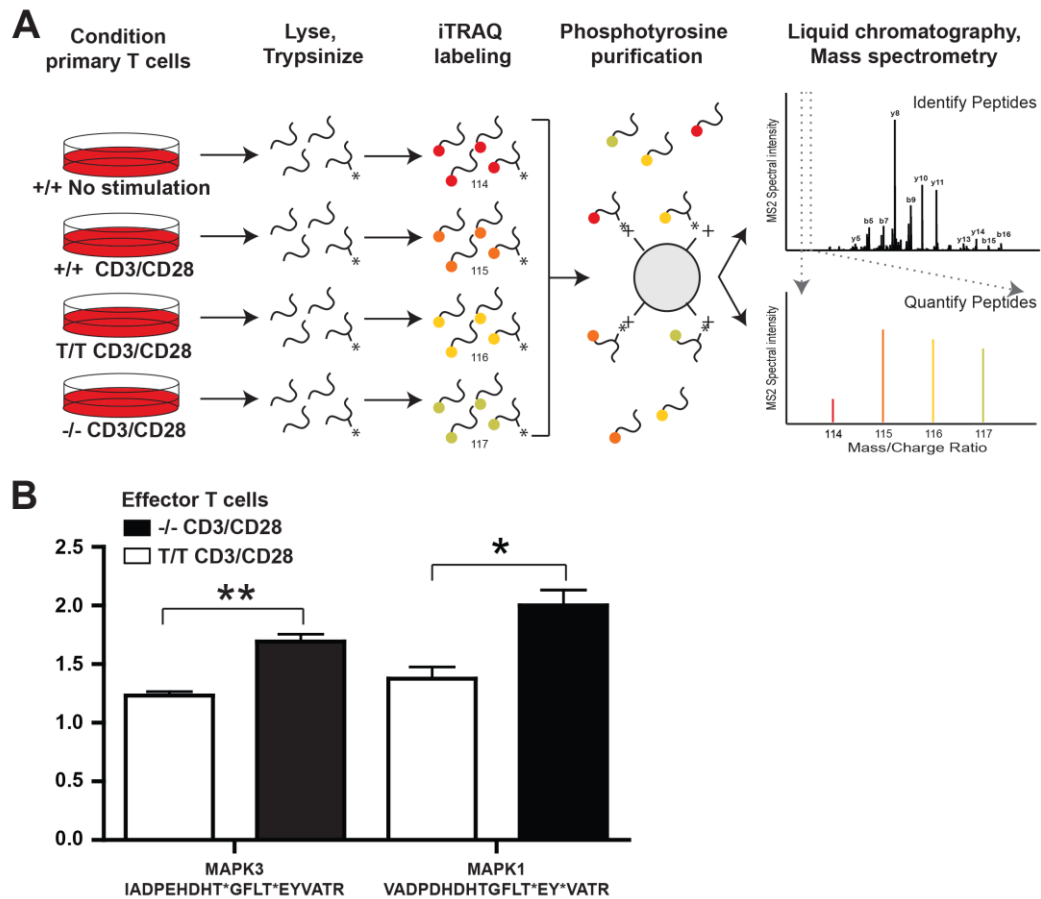
**Supplemental Figure 9. Expansion of memory/effector T cells in aged PEP-R619W knock-in mice.** (A) Increased of CD8<sup>+</sup> memory/effector T cells in aged T/C, T/T vs. WT littermates. Splenocytes or lymph node (LN) cells from aged (6 mo) mice were analyzed by FACS using anti-CD4, -CD8, -CD44 and -CD62L staining. Percentages indicate cells within the CD4<sup>+</sup> gate (left). Absolute numbers of naïve and memory/effector CD8<sup>+</sup> (right). Error bars represent standard deviation based on 8 animals/genotype; \* p<0.05. (B) CD4<sup>+</sup> and CD8<sup>+</sup> T cells from aged T/T mice exhibit increased expression of T cell activation markers. Splenocytes from 6 mo animals were analyzed by FACS using anti-CD4, -CD8, -CD95, -CD69, -CD122 and -CD80 antibodies. Data are representative of eight (A) and three (B) independent experiments.



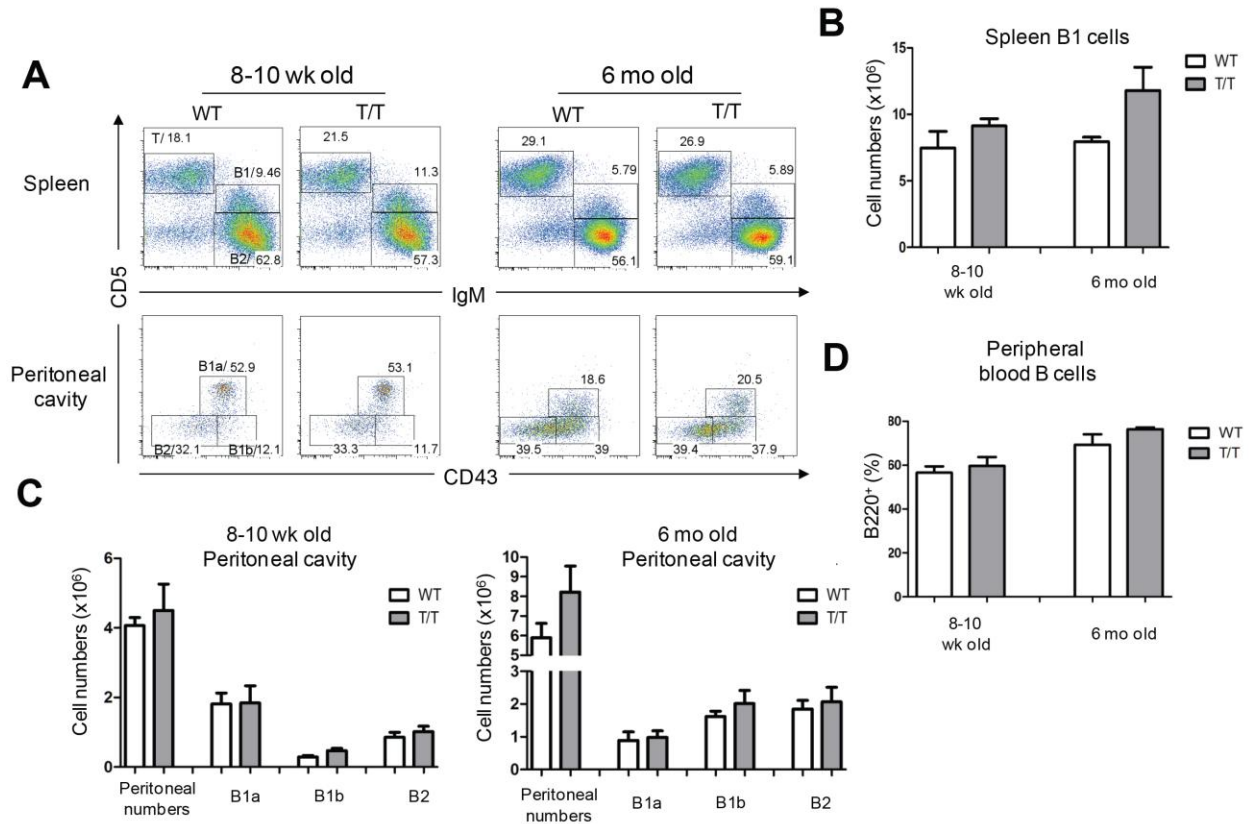
**Supplemental Figure 10. PEP-R619W expression does not impair Treg development or suppressive activity.** (A) Percentages of FoxP3<sup>+</sup> Treg in CD4<sup>+</sup> gated splenocytes and absolute numbers of Treg in spleen. Splenocytes from young (6-8 wk old, upper panels) and aged (6 mo, lower panels) T/C, T/T and littermate control mice were analyzed by FACS using anti-CD4 and -FoxP3 intracellular staining. Error bars indicate standard deviation based on 5 mice/genotype. (B) Control and T/T Treg exhibit similar suppressive activity. CD4<sup>+</sup>CD25<sup>-</sup>CD62L<sup>hi</sup> naïve T cells (Teff) and CD4<sup>+</sup>CD25<sup>+</sup> cells (Treg) were isolated from control or T/T mice, labeled with CellTrace and co-cultured with either control or T/T Treg at the indicated cell ratios in the presence of irradiated control APCs. Cells were cultured with 5µg/ml anti-CD3 for 3 days and cell proliferation was assessed by CellTrace dilution. Numbers indicate percentage of divided cells. Data shown is representative of five (A) and three (B) independent experiments.



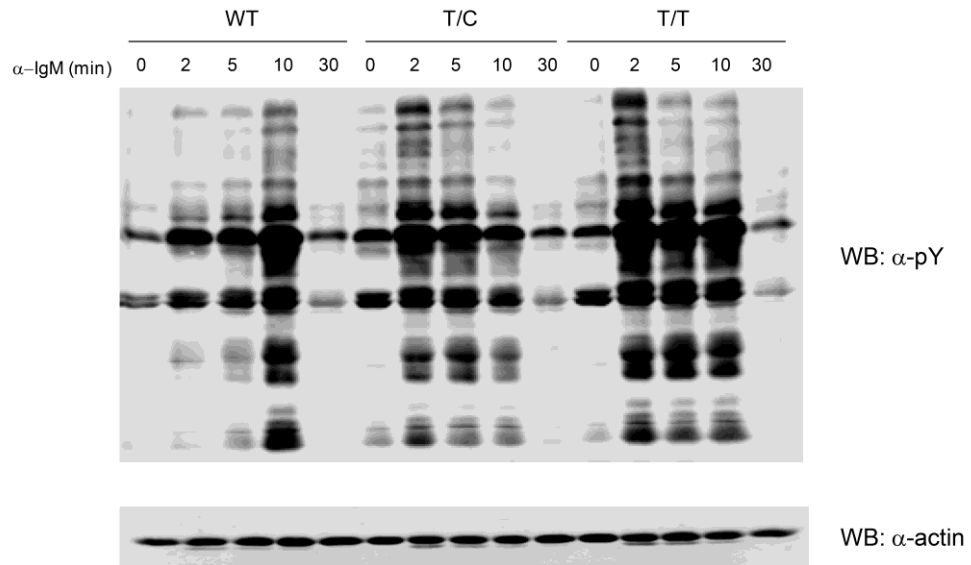
**Supplemental Figure 11. TCR, BCR and CD22 expression on T and B cells.** (A) Analysis of CD3 expression on naïve and memory/effector CD4<sup>+</sup> T cells. Splenocytes from 8-10 wk (upper panel) or 6 mo mice (lower panel) were analyzed by FACS using anti-CD4, -CD8, -CD44, -CD62L and -CD3 antibodies and CD3 mean fluorescence intensity (MFI) is displayed for gated T cell subsets. Error bars represent standard deviation (4 mice/genotype/age). (B) Analysis of IgM surface expression on splenic FM B cells. Splenocytes from 8-10 wk (upper panel) or 6 mo mice (lower panel) mice were analyzed by FACS using anti-B220, -CD21, -CD24, and -IgM antibodies and IgM MFI on gated FM B cells is displayed. Error bars represent standard deviation (4 mice/genotype/age). (C) Analysis of CD22 expression on mature BM B cells. BM cells from 8-10 wk or 6 mo mice were analyzed by FACS using anti-B220, -IgM, -IgD, and -CD22 antibodies and CD22 MFI on mature B cells is displayed. Error bars represent standard deviation (4 mice/genotype/age).



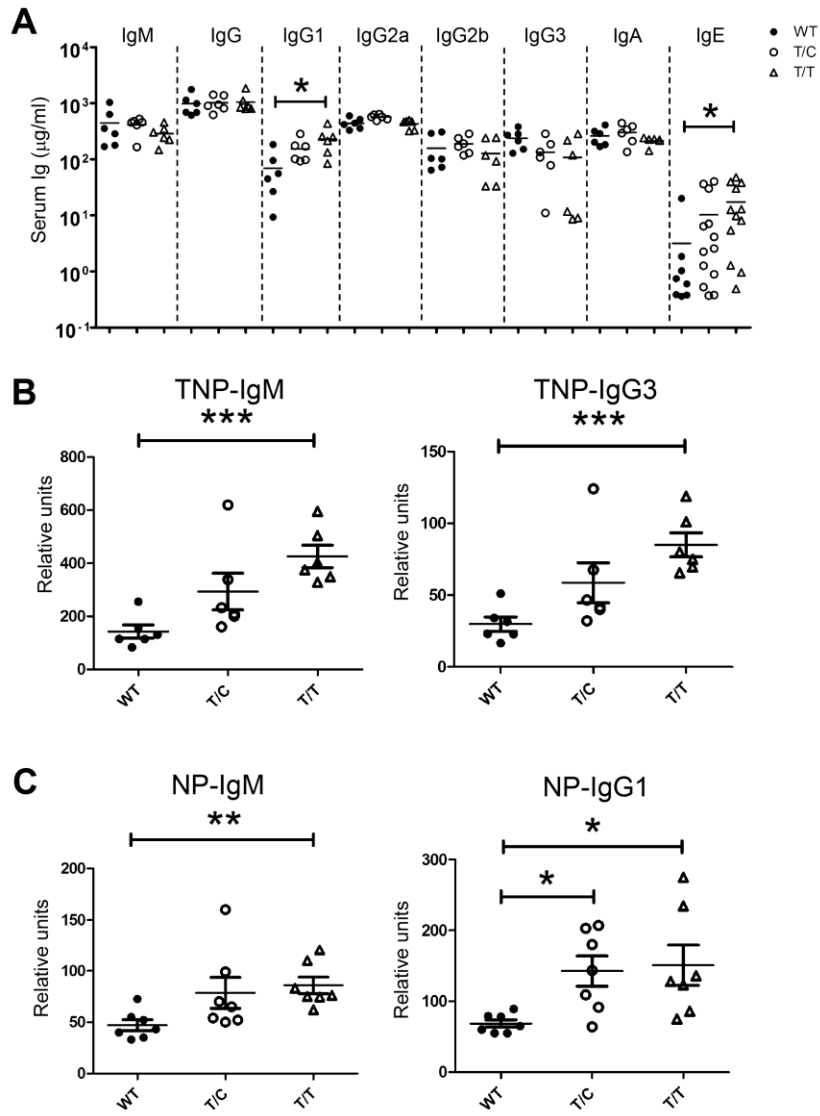
**Supplemental Figure 12. Phospho-proteome analysis of CD3/CD28-dependent signaling in *in vitro* generated T cells.** (A) Schematic of phosphoproteome analysis. *In vitro* generated T cells derived from T/T, PEP- deficient and control mice were stimulated for 5 min with anti-CD3 and anti-CD28. Following lysis and trypsinization, peptides isolated from each genetic background were labeled with different iTRAQ reporters. Labeled peptides were subsequently mixed and tyrosine phosphorylated peptides were isolated by protein G beads (Sigma) conjugated with a mixture of three anti-phosphotyrosine antibodies (pY100, Cell Signaling Technology; 4G10, Millipore; PT66, Sigma). Peptides were subsequently analyzed using high-resolution mass spectrometry. Detailed protocols for phospho-proteomic methods provided upon request. (B) Abundance of phospho-peptides corresponding to the activation loop of Mapk1 and Mapk3 isolated from T/T relative to those from PEP knock-out mice were plotted. Error bars represent standard deviation based on three samples for each genotype; \*  $p < 0.05$ ; \*\*  $p < 0.01$ .



**Supplemental Figure 13. PEP R619W does not alter B1 B cell or peripheral blood B cell populations.** (A-C) B1 B cell phenotype and absolute numbers in PEP-R619W knock-in mice. Splenocytes and peritoneal cells from 8-10 wk (left panels) or 6 mo (right panels) mice were analyzed by FACS using anti-B220, -CD5, -IgM, -CD19 and -CD43 antibodies. Subsets were defined as CD5<sup>lo</sup>IgM<sup>+</sup> (splenic B1), CD5<sup>lo</sup>IgM<sup>+</sup> (splenic B2), CD19<sup>+</sup>CD5<sup>lo</sup>CD43<sup>+</sup> (peritoneal B1a), CD19<sup>+</sup>CD5<sup>lo</sup>CD43<sup>+</sup> (peritoneal B1b) and CD19<sup>+</sup>CD5<sup>lo</sup>CD43<sup>-</sup> (peritoneal B2). Error bars represent standard deviation (4 mice/genotype/age). (D) Frequency of B cells in peripheral blood. Peripheral blood from 8-10 wk or 6 mo mice was analyzed by FACS using anti-B220 antibody. Error bars represent standard deviation (5 mice/genotype/age).



**Supplemental Figure 14. PEP R619W expression promotes enhanced tyrosine phosphorylation (pY) in response to BCR engagement in CpG pre-stimulated B cells.** CpG pre-stimulated B cells were stimulated with anti-IgM antibody for indicated times and cell lysates were blotted using an anti-pY antibody to measure activation and anti-actin as a loading control. Data shown is representative of two independent experiments.



**Supplemental Figure 15. Basal immunoglobulin (Ig) levels and T-independent and T-dependent immune responses in PEP-R619W knock-in mice.** (A) Increased IgG1 and IgE in aged PEP-R619W knock-in mice. Sera from aged T/C, T/T and littermate control mice (6 mo) were analyzed by ELISA for the indicated Ig isotypes. (B) Enhanced T-independent immune responses in knock-in mice. T/C, T/T and littermate control mice (6-8 wk old) were immunized with  $10\mu\text{g}$  TNP-Ficoll and sera were collected at Day 10 post-immunization. TNP-specific IgM and IgG3 were evaluated by ELISA. (C) Enhanced T-dependant immune responses in knock-in mice. T/C, T/T and littermate control mice (6-8 wk old) were immunized with  $100\mu\text{g}$  NP-CGG in alum and sera were collected at Day 14 post-immunization. NP-specific IgM and IgG1 were evaluated by ELISA. Each symbol represents an individual mouse, horizontal bars represent mean  $\pm$  SEM, \*  $p < 0.05$ ; \*\*  $p < 0.01$ , \*\*\*  $p < 0.001$ . Data shown is representative of two (B,C) independent experiments.

**Supplemental Table. Occurrence of characteristic lesions in various organs from aged T/C and T/T mice.**

Lesion site*	WT	T/C	T/T
Lung	0/4	4/6	6/6
Salivary gland	0/4	2/6	4/6
Bile and/or pancreatic ducts	0/4	1/6	5/6
Heart	0/4	1/6	2/6
Gastrointestinal tract	0/4	2/6	3/6

\*number of affected mice/total examined in each group.

Six homozygous (T/T), six heterozygous (T/C) and four WT littermate control mice (6 mo of age) were examined histologically for the presence of characteristic autoimmune lesions. Pulmonary lesions comprised striking vasculitic changes including perivascular cuffing with lymphocytic infiltrates, histiocytes, and neutrophils, intermittent disruption of the vascular wall and involvement of adjacent parenchyma. Targeted vessels included medium-large pulmonary arteries and veins as well as smaller vessels. Other tissues contained accumulations of lymphoid cells and/or mild vascular lesions. Salivary glands exhibited widely scattered, dense lymphoid foci that displaced parenchymal tissues. The gastrointestinal tract displayed vascular lesions accompanied by pyogranulomatous and necrotic elements suggesting secondary microbial involvement. While lesions were more frequent in T/T mice the nature of lesions was fundamentally similar to those seen in T/C mice. Wild type mice lacked lesions in all organs examined.

## SUPPLEMENTAL METHODS

**Generation of PEP-R619W knock-in and Rosa PEP-R619W knock-in mice.** The R619W mutation was introduced on exon 14 of the murine *Ptpn22* locus by site-directed mutagenesis using the strategy displayed in Supplemental Figure 1A. A loxP-flanked gene encoding neomycin resistance was used for positive selection and a gene encoding diphtheria toxin A was used for negative selection. The linearized targeting construct was electroporated into 129 ES cell lines expressing a protamine-Cre transgene. ES cells were screened by long-PCR and confirmed by Southern blot analysis. Three targeted embryonic stem (ES) clones were injected into C57BL/6J (B6) blastocysts. Male chimeras that transmitted the targeted knock-in allele expressed the Cre gene in their sperm and the floxed Neo was deleted in most germline F1 mice. Two clones gave rise to germline transmission and produced similar phenotypes. The presence of mutation was confirmed by sequencing RT-PCR products. The PEP-R619W knock-in mice were backcrossed two generations to B6 unless stated otherwise.

To generate Rosa PEP-R619W knock-in mice, a cDNA encoding N-terminal HA-tagged PEP-R619W and *cis*-linked GFP using a 2A-linked self-cleaving linker, preceded by a loxp flanked STOP-cassette, was cloned into pROSA26PA targeting vector provided by S. Srinivas (Oxford University, Oxford, UK). The linearized targeting construct was electroporated into 129 ES cell lines. ES cells were screened by long-PCR and confirmed by Southern blot analysis. The targeted embryonic stem (ES) clones were injected into B6 blastocysts. The chimeras were bred with B6 for one generation. The Rosa PEP-R619W mice were crossed with B6.129P2(C)-Cd19<sup>tm1</sup>(cre)Cgn/J (CD19 Cre; The Jackson Laboratory) to induce expression of PEP-R619W and GFP solely in B cells.

PEP-R619W knock-in mice and Rosa PEP-R619W knock-in mice were generated at Rodent Experimental Models (Boston, MA) or at the University of Washington Transgenic Resources Program, respectively.

**Flow cytometry.** Single-cell suspensions of various lymphoid organs were treated with ACK to lyse red blood cells and resuspended in PBS containing 2% FBS. The cells were then stained with

combinations of the following monoclonal antibodies conjugated to Fluorescein (FITC), phycoerythrin (PE), phycoerythrin/Cy7 (PE/Cy7), Peridin-Chlorophyll/Cy5.5 (PerCP/Cy5.5), allophycocyanin (APC), allophycocyanin/Cy7 (APC/Cy7), or biotin: anti-B220 (103236), anti-CD24 (101808), anti-CD21 (123411), anti-CD22 (126105), anti-CD5 (100605), anti-CD44 (103027), anti-CD4 (100434) and anti-CD122 (123207) were from BioLegend; anti-CD3 (25-0031), anti-CD38 (17-0381), anti-CD8 (12-0081), anti-CD62L (17-0621), anti-CD11b (12-0112), anti-CD11c (17-0114) and anti-CD25 (12-0251) were from eBioscience; anti-CD43 (553269), anti-CD69 (552879), anti-CD80 (553769) and anti-CD95 (554258) were from BD Biosciences; anti-IgM (A21238) was from Invitrogen; anti-IgD (1120-09) was from Southern Biotech; anti-PNA (FL-1071) was from Vector Labs; anti-M167 was generated as previously described(33). FoxP3 intracellular staining was performed using the Foxp3/Transcription Factor Staining Buffer Set (eBioscience). The stained samples were collected on LSRII cytometry (BD Biosciences) and data were analyzed using FlowJo software (TreeStar Inc).

***In vitro* Treg suppression assay.** Pooled splenic and lymph nodes CD4<sup>+</sup> T cells from F5 mice (backcrossed onto C57BL/6 background for 5 generations) were purified by the negative selection with CD4<sup>+</sup> T Cell Isolation Kit II (Miltenyi Biotech). The enriched CD4<sup>+</sup> T cells were stained with anti-CD4, -CD25 and -CD62L, and naïve CD4<sup>+</sup> (CD4<sup>+</sup>CD25<sup>-</sup>CD62L<sup>hi</sup>) T cells or Treg (CD4<sup>+</sup>CD25<sup>+</sup>) were sorted by FACS Aria (BD Biosciences). The naïve CD4<sup>+</sup> T cells were labeled with CellTrace (Life Technologies), co-cultured with Treg at various ratios in the presence of irradiated WT APCs. Cells were stimulated with 5µg/ml anti-CD3 for 3 days and cell proliferation was assessed by CellTrace dilution.

**OVA immunization.** Six to eight week old of mice were immunized s.c. on the lower back with 100µg EndoFit OVA (InvivoGen) emulsified in CFA. One week later, splenocytes from three mice of each genotype were stimulated individually with 10µg/ml OVA<sub>323-339</sub> (InvivoGen) for one day. Supernatants were collected and IL-2 production was measured using a murine IL-2 ELISA kit (eBioscience).

**FACS analysis of apoptosis (TUNEL assays).** Total splenocytes from 6-8 wk old mice were stained with anti-B220, -CD21 and -CD24, then fixed, permeabilized, and labeled according to

the manufacturer's instructions (*In Situ* Cell Death Detection kit, Roche Applied Science). After washing, the cells were collected on LSRII cytometry (BD Biosciences) and data were analyzed using FlowJo software (TreeStar Inc).

**Phospho-proteomic analysis of *in vitro* generated T cells.** *In vitro* generated effector T cells ( $20 \times 10^6$  per time point) were starved in 2% FBS RPMI media for 2 h, and then incubated on ice for 15 min with 10 $\mu$ g/ml anti-CD3 plus anti-CD28 followed by incubation of 10 $\mu$ g/ml goat anti-hamster IgG (Jackson ImmunoResearch). Cells were stimulated for 5 min at 37°C and lysed on ice with 3 ml of 8 M urea supplemented with 1 mM Na<sub>3</sub>VO<sub>4</sub>. A 10- $\mu$ l aliquot was taken from each sample to perform bicinchoninic acid protein concentration assay (Pierce) according to the manufacturer's protocol. Cell lysates were reduced with 10 mM DTT for 1 h at 56 °C, alkylated with 55 mM chloroacetamide for 30 min at room temperature, and diluted to 12 ml with 100 mM ammonium acetate, pH 8.9. 40  $\mu$ g of trypsin (Promega) was added to each sample (~100:1 substrate/trypsin ratio), and the lysates were digested overnight at room temperature. The whole-cell digest solutions were acidified to pH 3 with acetic acid (HOAc) and loaded onto C18 Sep-Pak Plus Cartridges (Waters). The peptides were desalted (10 ml of 0.1% HOAc) and eluted with 10 ml of a solution composed of 25% acetonitrile (MeCN) with 0.1% HOAc. Each sample was divided into 4 aliquots and lyophilized overnight to dryness for storage at -80 °C.

Peptide labeling with the 8-plex iTRAQ reagent (AB Sciex) was performed according to the manufacturer's protocol. Three aliquots (approximately  $2 \times 10^7$  cells per labeling) were dissolved in a total of 30  $\mu$ L of 0.5M triethylammonium bicarbonate, pH 8.5. The peptide mixtures were mixed with 1 tube of iTRAQ reagent that was previously dissolved in 70 $\mu$ L ethanol. The labeling reaction was carried out for 60 minutes at room temperature, and the ethanol was subsequently removed by dehydration. Eight samples that were labeled with the different iTRAQ reagents were combined and dissolved in 400  $\mu$ L immunoprecipitation buffer (100 mM Tris HCl, 0.3% NP-40, pH 7.4). The sample was then incubated overnight at 4 °C with 12  $\mu$ g each of three phospho-Tyrosine antibodies (pY100, Cell Signaling Technology; 4G10, Millipore; PT66, Sigma) previously conjugated to Protein G beads (Sigma). Following three washes with immunoprecipitation buffer, the phospho-Tyrosine containing peptides were eluted by incubation with 0.1% trifluoroacetic acid (Sigma).

Phospho-Tyrosine containing peptides were loaded onto a 10-cm self-packed C18 capillary precolumn (POROS RL2 10 $\mu$ M beads, inner diameter, 100  $\mu$ m; outer diameter, 360  $\mu$ m). After a 10-min rinse (0.1% HOAc), the precolumn was connected to a 20-cm self-packed C18 (Moniter 5  $\mu$ M) analytical capillary column (inner diameter, 50  $\mu$ m; outer diameter, 360  $\mu$ m) with an integrated electrospray tip ( $\sim$ 1- $\mu$ m orifice). Online peptide separation followed by mass spectrometric analyses was performed on a 2D-nanoLC system (nanoAcquity UPLC system, Waters Corp.). Peptides were eluted using a 120-min gradient with solvent A (H<sub>2</sub>O/Formic Acid, 99.9:1 (v/v)) and B (Acetonitrile/Formic Acid, 99.9:1 (v/v)): 10 min from 0% to 10% B, 75 min from 10% to 40% B, 15 min from 40% to 80% B, and 20 minutes with 100% A. Eluted peptides were directly electrosprayed into a LTQ Orbitrap Velos mass spectrometer (Thermo Fisher Scientific) equipped with a high energy collision cell.

The mass spectrometer was operated in a data-dependent mode to automatically switch between MS and MS/MS acquisitions. Each full scan (from  $m/z$  300-1500) was acquired in the Orbitrap analyzer (resolution = 60,000), followed by MS/MS analyses on the top seven most intense precursor ions that had charge states greater than two. For each full scan, we performed seven low energy collision induced dissociation (CID) MS/MS scans followed by seven high collision induced dissociation (HCD) MS/MS spectra (in each case we scanned from  $m/z$  100-1700). The HCD MS/MS scans were acquired using the Orbitrap system (resolution = 7,500) at normalized collision energy of 60% and the CID MS/MS scans were scanned in a low pressure ion trap with a normalized collision energy of 35%. The precursor isolation width was set at 1.5  $m/z$  for each MS/MS scan and the maximum ion accumulation times were as follows: MS (500 mS), HCD MS/MS (250 mS), and CID (25 mS).

MS/MS data files were first processed using the Tagtraq algorithm (The University of Washington's Proteomic Resource Facility, 2011), which merges HCD and CID MS/MS scans into one scan associated with each precursor ion and converts the files to .mzXML. The merged mzXML files were searched using the SEQUEST algorithm (The University of Washington's Proteomic Facility, 2011) and the output was imported into the 'Trans-Proteomic Pipeline' (Institute for Systems Biology (1)). The following variable (Phosphorylation of Serine, Threonine or Tyrosine; 79.8 Da) and static (carbamidomethylation of Cysteine; 57.02 Da, and iTRAQ labeling to N-terminus and Lysine; 304.2 Da) modifications were used in the search. All

identified peptides whose peptide probability score exceeded the peptide probability score associated with a <2.5% false discovery rate were retained.

Peptide quantification based on the iTRAQ labels was performed using the LIBRA software embedded in the Trans-Proteomic Pipeline (2). The intensity of the label associated with one of the wild type anti-CD3/CD28 stimulated samples was used to calculate the ratios of the other reporter ions. As this sample was included in all of our independent experiments, it allowed normalization across experiments. To normalize for variability in the labeling or input protein amounts, the reporter ions for the phospho-tyrosine immunoprecipitated peptides was further normalized to the averages of all unphosphorylated peptides corresponding several highly expressed proteins which we expect to remain at constant abundance across conditions (Vim, Tubb2b, Eef1a1, Tuba1b, Acta1, Actb, and Hspa8).

For visualization of interactions inferred from our mass spectrometry data and those curated from the literature between proteins involved in T cell receptor signaling, we used the Cytoscape visualization software (3) and the MultiColoredNodes Plugin (4).

### Supplemental References

1. Deutsch, E.W., Mendoza, L., Shteynberg, D., Farrah, T., Lam, H., Tasman, N., Sun, Z., Nilsson, E., Pratt, B., Prazen, B., et al. 2010. A guided tour of the Trans-Proteomic Pipeline. *Proteomics* 10:1150-1159.
2. Pedrioli, P.G., Raught, B., Zhang, X.D., Rogers, R., Aitchison, J., Matunis, M., and Aebersold, R. 2006. Automated identification of SUMOylation sites using mass spectrometry and SUMmOn pattern recognition software. *Nat Methods* 3:533-539.
3. Shannon, P., Markiel, A., Ozier, O., Baliga, N.S., Wang, J.T., Ramage, D., Amin, N., Schwikowski, B., and Ideker, T. 2003. Cytoscape: a software environment for integrated models of biomolecular interaction networks. *Genome Res* 13:2498-2504.
4. Warsow, G., Greber, B., Falk, S.S., Harder, C., Siatkowski, M., Schordan, S., Som, A., Endlich, N., Scholer, H., Repsilber, D., et al. 2010. ExprEssence--revealing the essence of differential experimental data in the context of an interaction/regulation network. *BMC Syst Biol* 4:164.